

MI Microglia-Derived Exosomes Promote A1 Astrocyte Activation and Aggravate Ischemic Injury via circSTRN3/miR-331-5p/MAVS/NF- κ B Pathway

Zhongyuan Li^{1,*}, Pengfei Xu^{2,*}, Yang Deng^{3,*}, Rui Duan¹, Qiang Peng¹, Shiyao Wang¹, Zhaohan Xu¹, Ye Hong¹, Yingdong Zhang¹

¹Department of Neurology, Nanjing First Hospital, Nanjing Medical University, Nanjing, 210000, People's Republic of China; ²Department of Neurology, The First Affiliated Hospital of USTC, Division of Life Sciences and Medicine, University of Science and Technology of China, Hefei, Anhui, 230001, People's Republic of China; ³Department of Neurology, Nanjing First Hospital, China Pharmaceutical University, Nanjing, 210006, People's Republic of China

*These authors contributed equally to this work

Correspondence: Ye Hong; Yingdong Zhang, Department of Neurology, Nanjing First Hospital, Nanjing Medical University, No. 68, Changle Road, Nanjing, 210000, People's Republic of China, Email dg1735053@smail.nju.edu.cn; zhangyingdong@aliyun.com

Background: After ischemic stroke (IS), microglia and astrocytes undergo polarization, transforming into a pro-inflammatory phenotype (M1 or A1). According to previous studies, exosomes might play an important role in the interplay between M1 microglia and A1 astrocytes after IS.

Methods: We used the microglial oxygen-glucose deprivation/reperfusion (OGD/R) model and ultracentrifugation to extract M1 microglial exosomes (M1-exos). Subsequently, we identified circSTRN3 enriched in exosomes through RNA sequencing and detected the role of circSTRN3 in astrocyte activation based on bioinformatics analysis, immunofluorescence, Western blotting, and polymerase chain reaction analysis. We validated these findings in the middle cerebral artery occlusion/reperfusion (MCAO/R) model of adult male C57BL/6J mice. Finally, we confirmed the correlation among circSTRN3, miR-331-5p, and stroke severity score in exosomes isolated from peripheral blood of IS patients.

Results: Our findings revealed that M1-exos promoted A1 astrocyte activation. CircSTRN3 was abundant in M1-exos, which could sponge miR-331-5p to affect mitochondrial antiviral signaling protein (MAVS), activate NF- κ B pathway, and participate in A1 astrocyte activation. In addition, overexpressed circSTRN3 augmented the infarct size and neurological dysfunction in MCAO/R models, while miR-331-5p mimics reversed the effect. Furthermore, circSTRN3 in IS patients was positively correlated with stroke severity score ($R^2 = 0.83$, $P < 0.001$), while miR-331-5p demonstrated a negative correlation with the same score ($R^2 = 0.81$, $P < 0.001$).

Conclusion: Taken together, our research indicated that circSTRN3 from M1-exos could promote A1 astrocyte activation and exacerbate ischemic brain injury via miR331-5p/MAVS/NF- κ B axis.

Keywords: ischemic stroke, microglia, astrocyte, exosome, circSTRN3, miR-331-5p

Introduction

Ischemic stroke (IS) is a highly destructive central nervous system disease.¹ According to previous studies, IS has become the second largest cause of mortality worldwide.² Focal hypoperfusion rapidly activates the process of oxidative stress and neuroinflammation response through producing pro-inflammatory factors after IS.³ On the one hand, neuroinflammation facilitates the removal of dead and dying tissues and cells.⁴ On the other hand, neuroinflammation can trigger the release of neurotoxins, compromise blood brain barrier (BBB) integrity and exacerbate ischemic injury.⁵⁻⁷ Nevertheless, the further mechanism of neuroinflammation progressing during IS is still unknown.

Microglia and astrocytes, being two vital components of glial cells, play an essential role in the progression of neuroinflammation during IS.⁸ Microglia engage in immune response by adopting two distinct phenotypes: the pro-inflammatory M1 phenotype and the anti-inflammatory M2 phenotype.⁹ According to previous literature, M1 microglia are related to up-regulated inflammatory factors like CD86, iNOS and tumor necrosis factor- α (TNF- α), while M2 microglia are related to anti-inflammatory Arginine-1 (Arg1), CD206 and CD10.^{10–13} Several studies have demonstrated that transforming microglia from M1 to M2 helps decrease neuroinflammation and ischemic injury.^{14,15} Likewise, under exogenous or endogenous stimuli, astrocytes will also differentiate into pro-inflammatory A1 phenotype to involve in the regulation of inflammation.^{16,17} For example, after infection or metabolic disorder, mitochondrial antiviral signaling protein (MAVS) can activate A1 astrocytes through NF- κ B pathway to enhance neuroinflammation.¹⁸ Recent studies have suggested a close relationship between polarization of astrocytes and microglia, but the specific mechanism is still in the mist.

Exosomes are a class of vesicles composed of lipid bilayer membranes with a diameter of 30–150nm.¹⁹ Besides functional contents such as DNA, proteins and metabolites, exosomes can transfer abundant non-coding RNAs like circular RNAs (circRNAs) and microRNAs(miRNAs).^{20,21} Exosomes function in cell-signaling transmission and are intricately involved in regulating a number of diseases like amyotrophic lateral sclerosis, glioblastoma and Alzheimer's disease.^{22–24} In IS, it has been reported that exosomes from fat tissue-derived stem cells could improve functional recovery as well as repair nerve damage by shifting the microglia polarization.²⁵ Therefore, we supposed that exosomes derived from M1 microglia (M1-exos) might facilitate the polarization of A1 astrocytes after IS.

CircRNAs represent a unique class of single-stranded non-coding RNAs, which lack a 5' cap or 3' poly(A) tail and have the covalently loop-locked structure instead.^{26,27} CircRNAs are thought to regulate neuronal function, cell proliferation, and innate immunity.²⁸ Recent studies showed that circRNAs were abundant with miRNA binding sites, which could function as a miRNA sponge, thereby attenuating the inhibition of miRNAs on their target genes and increasing the expression level of target genes.²⁹ For example, circRNA0025984 was reported to decrease ischemic damage and protect astrocytes via miR-143-3p/TET1/ORP150 pathway.³⁰ Also, circSTRN3 described in our research was reported to aggravate inflammation in acute kidney injury through miR-578/toll-like-receptor-4 (TLR4) axis.³¹ MiR-331-5p was reported to be downregulated in mice middle cerebral artery occlusion/reperfusion (MCAO/R) models and could help inhibit inflammation after ischemic injury.³² Therefore, we assumed that circSTRN3 could sponge miR-331-5p to involve in A1 astrocyte activation.

Our research used oxygen-glucose deprivation/ reoxygenation (OGD/R) in primary astrocytes and MCAO/R models in C57BL/6J mice. In order to demonstrate whether M1-exos-derived circSTRN3 could induce A1 astrocyte activation and aggravate ischemic injury through miR-331-5p/MAVS/NF- κ B axis. Our study shed light on a new target for IS therapy strategy.

Materials and Methods

Experimental Animals

The adult male C57BL/6J mice (25–30 g, 8–10 weeks) were all sourced from Charles River Company (Beijing, China). They were housed in a controlled environment with 6 mice per cage, at a temperature of $22 \pm 2^\circ\text{C}$ and humidity of 50–60%. A 12-hour light-dark cycle was observed, and the mice had unrestricted access to food and water. All experimental procedures were approved by the Ethics Committee of Nanjing First Hospital (Approval No. DWSY-23146450) and were conducted in strict adherence to the National Institutes of Health (NIH) Guidelines for the Care and Use of Laboratory Animals³³ (NIH Publication No. 80–23, revised 1996). Mice were randomly assigned to groups and treated; investigators were blinded to group assignment.

Animal Clusters

We segregated the experimental mice into two distinct sets. In the first set, sham operation and MCAO were performed on mice to confirm the activation sequence of A1 and A2 astrocytes following MCAO/R. After surgery, MCAO mice would survive for 1, 3, 5, or 7 days and then their brains were extracted for immunofluorescence assays. The second set of mice were split into 4 groups, including Sham, MCAO/R+OE+NC mimic (MCAO/R group), MCAO/R+OE-circSTRN3+NC mimic (OE-circSTRN3 group) and MCAO/R+OE-circSTRN3+miR-331-5p mimic (OE-circSTRN3

+miR-331-5p mimic group) to verify the circSTRN3/miR-331-5p/MAVS/NF- κ B pathway in MCAO/R models. Mice in MCAO/R group underwent intracerebroventricular injection with control lentivirus and NC mimic using a stereotaxic apparatus (RWD, Shenzhen, China) before surgery. Similarly, mice in OE-circSTRN3 group were injected with overexpressed circSTRN3 lentivirus (GeneChem, Shanghai, China) and NC mimic. Mice in OE-circSTRN3+miR-331-5p mimic group were injected with overexpressed circSTRN3 lentivirus (GeneChem, Shanghai, China) and miR-331-5p mimic (GenePharma, Shanghai, China). These mice underwent MCAO 72 h after injection. They were detected with neurological severity score and behavioral tests at 1, 3 and 5 d after the operation. At last, their brains were extracted for next experiments.

MCAO/R Model

About 2% isoflurane in O₂ (RWD Life Science, Shenzhen, China) was used to anaesthetize mice to render them unconscious. A surgical incision was carefully performed along the midline of the neck to expose the right common carotid artery (CCA), external carotid artery (ECA), and internal carotid artery (ICA). After securely ligating the CCA and the ECA, a silicone-coated monofilament (diameter: 0.18 ± 0.01 mm; Cinotech, Beijing, China) was gently inserted from ECA into ICA until a subtle resistance was encountered. This monofilament was then withdrawn 1 hour later to induce reperfusion. Throughout the surgical procedure, the body temperature of mice was maintained at $37 \pm 0.5^\circ\text{C}$ with the heating pad. In addition, an identical surgical process was performed on sham-operated mice without inserting the monofilament.³³

Immunofluorescence Assays

Firstly, mice brain tissues were cut into 4 μm -thick sections after being embedded in paraffin. After deparaffinizing by xylene and rehydrating with ethanol of gradient concentrations from 100% to 50%, sections were set into sodium citrate buffer to fix the antigen. Following a 30-minute permeability period at ambient temperature with 0.1% Triton X-100 (Beyotime, Shanghai, China) in phosphate buffered saline (PBS), 5% BSA (Biofroxx, Shanghai, China) was used to block tissue sections for 1 h. Next, anti-C3 (1:100, sc-28294, Santa Cruz Biotechnology, Texas, USA), anti-S100A10 (1:100; 11,250-1-AP, Proteintech, Wuhan, China) and GFAP (1:100, ab7260, Abcam, Cambridge, UK) were added to sections for incubation overnight at 4 °C. Following three washes in PBS, conjugated secondary antibodies was applied and incubated at room temperature for one hour. Finally, DAPI (C1002, Beyotime, Shanghai, China) was used to stain nuclei for five minutes and the immunofluorescence results were observed by a fluorescence microscope (Zeiss, Oberkochen, Germany).³⁴ For the immunofluorescence assays of primary astrocytes, cells were fixed by 4% paraformaldehyde and blocked with 0.2% bovine serum albumin for 30 minutes. The subsequent staining steps of anti-C3 and anti-GFAP antibodies were identical to those employed for the brain tissue.

Primary Astrocytes and Microglia Culture

After extracting the cerebral cortex of neonatal mice (aged 1–3 days), the meninges and blood vessels were stripped. After chopping and digesting with 0.125% trypsin (25200–056, Gibco, New York, USA), the cerebral cortical tissues were then filtered and centrifuged to obtain a mixture of primary glia cells. The mixture was cultured in the complete medium of DMEM/F12 (11320033, Gibco, New York, USA). Every 3 days the medium was changed to remove impurities and dead cells. Approximately 2 weeks later, astrocytes and microglia would grow abundantly and spread over the bottom of the culture flask. Subsequently, the cells underwent 260-rpm oscillation at 37°C for 16h. The detached microglia were collected and cultured in the complete medium of DMEM (11995065, Gibco, New York, USA) while the remained astrocytes were still cultured in DMEM/F12 complete medium. Microglia and astrocytes were cultured in a 37°C and 5% CO₂ humidified incubator. All complete mediums were added with 10% fetal bovine serum (FBS) (10100147, Gibco, New York, USA) and 1% penicillin/streptomycin (15140122, Gibco, New York, USA).³³

OGD/R Model

Briefly, primary microglia were cultured with a glucose-free DMEM medium (11966025, Gibco, New York, USA) without FBS in a hypoxia chamber with 95% N₂ and 5% CO₂ for 4h according to our previous study.³⁴ For reoxygenation, cells were subsequently cultured with a DMEM complete medium in the environment with 5% CO₂ in air for different durations of time.

The OGD/R model utilized for primary astrocytes remained identical, barring variations solely in the culture medium. The time of reoxygenation for astrocytes was 48h.

Western Blotting Analysis (WB)

Firstly, RIPA lysis buffer (89900, Thermo Fisher Scientific, CA, USA) was used to extract the protein from cells or tissues. Then, a BCA protein assay kit (23225, Thermo Fisher Scientific, CA, USA) was used to quantify proteins. The phosphatase inhibitor (P1096, Beyotime, Shanghai, China) was added to prevent phosphorylated proteins from degrading. The sodium dodecyl-sulfate–polyacrylamide gel electrophoresis was utilized to separate samples (30–40µg/lane) in the electrophoresis tank with appropriate voltage. Next, polyvinylidene difluoride (PVDF, Roche, Basel, Switzerland) membranes were used to transfer proteins, in which the duration time was determined by the molecular weight of the target protein. After 1-hour blocking with 5% defatted milk, primary antibodies against CD206 (1:1000; 18,704-1-AP, Proteintech, Wuhan, China), iNOS (1:1000; ab178945, Abcam, Cambridge, UK), C3 (1:10,000; 21,337-1-AP, Proteintech, Wuhan, China), S100A10 (1:1000; 11,250-1-AP, Proteintech, Wuhan, China), GFAP (1:1000; 3670, Cell Signaling Technology (CST), Boston, USA), p65 (1:1000; Ab32536, Abcam, Cambridge, UK), p-p65 (1:1000; ab76302, Abcam, Cambridge, UK), IκBα (1:1000; Ab32518, Abcam, Cambridge, UK), p-IκBα (1:10000; Ab133462, Abcam, Cambridge, UK), MAVS (1:5000; 66,911-1-Ig, Proteintech, Wuhan, China), CD63 (1:1000; ab217345, Abcam, Cambridge, UK), TSG101 (1:1000; ab125011, Abcam, Cambridge, UK), GM130 (1:1000; 70767, CST, Boston, USA), calnexin (1:5000; 10,427-2-AP, Proteintech, Wuhan, China) and β-actin (1:1000; 4970, CST, Boston, USA) were utilized to incubate membranes with a slight shaking overnight at 4°C. Followed by washing in tris-buffered saline and tween 20 (TBST, Biosharp Life Sciences, Beijing, China) for three times, corresponding secondary antibodies were used to incubate membranes at room temperature for 2h. Finally, after washing three times again with TBST, membranes were observed using an Enhanced Chemiluminescence Plus Kit (Thermo Fisher Scientific, CA, USA). The expression of target protein was quantitatively analyzed by ImageJ (National Institutes of Health, Maryland, USA).³⁴

Exosome Extraction and Identification

Exosomes were extracted by the method of differential centrifugation.³⁵ According to different treatment, microglia (be cultured to 90%) were divided into two groups: M0 with normal culture conditions and M1 with 4-hour OGD and 48h reoxygenation followed. Firstly, replace the DMEM complete medium of microglia with DMEM medium with 10% exosome-depleted FBS (EXO-FBS-50A-1, SBI, CA, USA) and 1% penicillin/streptomycin. Secondly, collect the supernatant from the culture medium and centrifuge at 300g, 2,000g and 10,000g in sequence to get rid of dead cells and debris. Thirdly, filter it through a 0.22µm filter (Millipore, MA, USA), and centrifuge at 100,000g for 70 minutes twice for precipitating. At last, dissolve exosomes with PBS. The collected exosomes were detected and visualized by a transmission electron microscope (FEI, Hillsboro, OR, USA) and the NanoSight NS500 instrument (NanoSight Technology, Malvern, UK) was utilized for nanoparticle tracking analysis (NTA). The expressions of CD63 and TSG101, regarded as exosome markers, were assayed by WB.

Exosome Uptake

In order to detect that exosomes were devoured by astrocytes, the isolated exosomes were labeled by the PKH26 (red) kit (Sigma-Aldrich, MO, USA) according to the manufacturer's protocol. Briefly, exosome samples were added into the dye mixture including of PKH26 labeling dye and reaction buffer and incubated for 30 minutes at 37°C. Then, the exosome mixture was added into a spin column and centrifuged with PBS buffer for purification. After filtering through 0.45µm filter membrane, the labeled exosomes were added into cultured primary astrocytes for 24h. The following steps were identical to the immunofluorescence assays for astrocytes. The anti-GFAP (1:500; 60,190-1-Ig, Proteintech, Wuhan, China) antibody was used to mark astrocytes. The uptake of exosomes was observed by a fluorescence microscope (Zeiss, Oberkochen, Germany).³⁶

Cellular and Tissue RNA Extraction

The extraction of cellular RNA adhered to a precise and detailed protocol.³⁷ Briefly, cells were lysed using a Trizol reagent (Thermo Fisher Scientific, CA, USA). RNAs were then precipitated with isopropanol following chloroform extraction. Then, the precipitated RNAs underwent washing with ethanol. After centrifugation, the samples were allowed to stand at room temperature to evaporate the ethanol. Finally, RNAs were dissolved in diethyl pyrocarbonate water (DEPC, Biosharp Life Sciences, Beijing, China). The extraction process for tissue RNAs followed a similar protocol, with the additional steps of homogenization and centrifugation in the initial phase.

CircRNA Sequencing

After isolating exosomes from M0 and M1 microglia, the TRIzol reagent (Thermo Fisher Scientific, CA, USA) was used to extract RNAs. The sequencing assays were supported by Ribobio Company (Guangzhou, China). Briefly, the raw data was filtered to remove splice sequences and low-quality reads. After removing ribosomal RNA sequences by utilizing ribosomal database, the effective reads were then obtained. Next, the effective reads were used for circRNA identification in comparison with the reference genome using two circRNA analysis toolsets, CIRI2 and CIRCexplorer. The identified circRNAs underwent rigorous sequence prediction, expression value calculation and differential expression analysis.³⁸ The screening criteria for differentially expressed circRNAs between the two groups, M0 and M1, was a $|\log_2\text{Fold change}| > 1$ and a P value < 0.05 . The sequencing data have been deposited in GenBank (GSE268852).

Quantitative Real-Time Polymerase Chain Reaction (qRT-PCR)

An Applied biosystems Real-time PCR System (7500, ABI, CA, USA) served as a platform for the PCR analysis of circSTRN3 and miR-331-5p.³⁴ Initially, total RNAs were extracted, followed by the removal of genomic DNA (gDNA) by a gDNA wiper. Subsequently, a PrimeScript RT Reagent (Perfect Real Time) Kit (Takara, Kyoto, Japan) was used to reverse transcribe RNAs. Next, the RT products were quantified using the TB Green Premix Ex Taq II (Tli RNaseH Plus) (Takara, Kyoto, Japan). The ABI7500 Real-time PCR System was used for the detection. The circRNA levels were normalized to β -actin, while miRNA was normalized to U6. The primers for amplifying circRNA and miRNA transcripts were synthesized by GenePharma Company (Shanghai, China).

Bioinformatic Analysis

The website (<https://bibiserv.cebitec.uni-bielefeld.de/rna>) was utilized to foretell the combination between circSTRN3 and miR-331-5p, while the potential combining targets of miR-331-5p and MAVS were meticulously examined using the online bioinformatics database TargetScan (<https://www.targetscan.org/>).

Dual-Luciferase Reporter Assays

Briefly, the luciferase reporter plasmids containing Wild-type (WT) and mutant (MUT) circSTRN3 (3'UTR) was constructed by GenePharma Company (Shanghai,China). Then, plasmids were co-transfected into HEK293T cells (National Collection of Authenticated Cells Cultures) using Lipofectamine 3000 (Invitrogen, Thermo Fisher Scientific, CA, USA) with NC mimic or miR-331-5p mimic respectively. Following a 48-hour incubation period, cells were harvested for lysis, and luciferase activity was quantified using the dual-luciferase reporting and detection system (Promega, WI, USA).³⁴ The same method was utilized to assay the combined effects of MAVS and miR-331-5p.

Cell Transfection and Lentivirus Infection

The miR-331-5p mimic, miR-331-5p inhibitor, and respective negative control (NC mimic, NC inhibitor) were purchased from Shanghai GenePharma Company (Shanghai, China) and transfected to primary astrocytes using Lipofectamine 3000 (Invitrogen, CA, USA). The lentiviruses loaded with shRNA were acquired from GeneChem Company (Shanghai, China), including overexpressed circSTRN3 (OE-circSTRN3), overexpressed MAVS (OE-MAVS) and their control lentivirus (OEC). Infecting lentivirus was carried out in a strict accordance with the manufacturer's protocol.

Neurological Severity Score and Behavioral Testing

The modified neurological severity scores (mNSS) test was used to evaluate the neurological function at 1, 3 and 5 days after MCAO/R,³⁹ which scored from 0 to 14. The score of 1–4 indicates mild injury; 5–9 was moderate injury; and 10 to 14 was severe injury. Behavioral tests were also carried out 1 day before MCAO/R and at 1, 3, 5 days after the surgery. The behavioral tests encompassed the corner test and the rotarod test, with the protocol grounded in prior research.⁴⁰ The corner test assessed sensory and motor impairments in mice and times mice and the number of times the mice turned right in the corner during 10 experiments was recorded. The rotarod test assessed the coordinated movement and balance ability of mice and the duration of time each mouse remained on the rod was recorded for analysis. Furthermore, neurological deficit assessment and behavioral tests were executed by two investigators, both of whom were unaware of the identities of the groups.

Triphenyl Tetrazolium Chloride Staining (TTC Staining)

TTC staining was carried out at 24h after the sham operation or MCAO/R. Briefly, mice brains were extracted, frozen for 5 min, and subsequently sliced into six sections, each with a thickness of 2mm. The sections started in the frontal lobe and excludes the brainstem and cerebellum. Then, the 2% TTC (17779, Sigma-Aldrich, USA) solution was used to stain sections at 37°C for 30 min. After staining, the sections were fixed using 4% paraformaldehyde. For the purpose of quantifying the percentage of normal tissues (identified as red regions) and infarction areas (identified as white regions), ImageJ software was employed.³⁴

Hematoxylin-Eosin Staining (HE Staining)

Firstly, mice underwent MCAO or sham operation were anesthetized with 2% isoflurane in O₂ at 24h after surgery. Then, normal saline (200mL) and 4% paraformaldehyde (200 mL) were perfused into the mice heart. The brains were then extracted and cut into 5- μ m thick sections. After preparing the paraffin sections, the sections were methodically submerged in xylene, followed by graded concentrations of ethanol, and ultimately stained with hematoxylin and eosin staining solution. Pathological changes were visualized by a light microscope (Zeiss, Oberkochen, Germany).³⁴

Human Plasma Collection

Between January and December 2023, IS patients admitted to the Department of Neurology at Nanjing First Hospital were enrolled in the study. All participants were diagnosed using a Magnetic Resonance Imaging (MRI) or a computed tomography scan of brain. The National Institute of Health Stroke Scale (NIHSS) was used to evaluate the severity of IS by two experienced neurologists within 24h after onset. Patients with the following diseases were excluded: malignant tumor, hematological system diseases, intracerebral hemorrhages, severe cardiac and renal insufficiency. All the plasma was collected within 24h after admission. These healthy controls (HC) without IS were recruited from individuals receiving annual medical examinations at the hospital. A total of 30 IS patients and 30 HC were enrolled in our study. Written informed consents were provided by all participants or their legally authorized representatives. This research has been approved by the Ethics Committee of Nanjing First Hospital (Approval No. KY20211011-05).

Plasma Exosome Extraction

An exosome extraction kit (Keygen Biotech, Jiangsu, China) was used to extract exosomes from plasma. Initially, blood samples underwent a centrifugation to isolate the plasma. Then, an exosome isolation reagent was added to the plasma and incubated for 2 h at 4°C. Following a centrifugation at 12000 g for 20 min, the exosomes were effectively precipitated. Next, the exosome RNA was isolated using an identical method for cellular RNA isolation. The purified RNA was stored at -80°C for experiments.

Statistical Analysis

Statistical analysis was conducted using GraphPad Prism 10 (GraphPad, San Diego, CA, USA). Data were expressed as the mean \pm standard deviation (SD), representing an aggregation of results from at least three independent experiments.

Prior to analysis, it was verified that all data followed a normal distribution, and the variances between groups were comparable. To assess the differences between groups, Student's *t* test was employed for comparisons between two groups, while one-way analysis of variance (ANOVA) was utilized for comparisons involving three or more groups. For the analysis of neurological severity score and behavioral tests, a two-way repeated-measures ANOVA was applied. The ANOVA analysis was followed by a Tukey's post hoc test. A meaningful difference between the groups was indicated by a *P* value of <0.05.

Results

M1 Microglia Activation Earlier Than A1 Astrocytes Activation

To confirm the activation of astrocytes, we investigated the expression level of C3 and S100A10 at 1, 3, 5 and 7 d after MCAO/R models. Immunofluorescence assays revealed that S100A10 levels increased between 1 to 3 days post MCAO/R, whereas C3 levels increased on the 5th day (Figure 1A–D). Comparable outcomes were observed in WB (Supplementary Figure S1A–D), suggesting that A2 astrocytes were activated earlier than A1 astrocytes. According to our previous research, M1 microglia were activated at 3 d after MCAO/R,⁴¹ which indicated that M1 microglia were activated earlier than A1 astrocytes after IS.

OGD/R Induced M1-Exos Promoted A1 Astrocytes Activation

To determine whether M1-exos could promote A1 astrocyte activation, we first extract and identify the exosomes from M1 microglia. At 48 h after OGD/R, M1 microglia was activated and M2 microglia decreased so that we chose 48h as the time point of M1-exos extraction (Figure 2A). The transmission electron microscopy results showed the extracts performed as oval vesicles (Figure 2B). The NTA revealed that the vesicles exhibited a size range of 30–150nm (Figure 2C). Next, the expression of CD63 and TSG101 were detected, which were positive markers for exosomes (Figure 2D). The exosome negative markers, GM130 and calnexin, were also tested (Supplementary Figure S2). According to the immunofluorescence results, we verified exosomes could be devoured by primary astrocytes (Supplementary Figure S3). Furthermore, we added M0-exos (exosomes from primary microglia) and M1-exos to primary astrocytes respectively. After adding M1-exos, primary astrocytes could be activated to A1 phenotype (Figure 2E). Compared to M0-exos, the addition of M1-exos increased the protein expression level of NF-κB pathway and C3, which served as active markers of A1 astrocytes (Figure 2F–I). These results showed M1-exos could promote A1 astrocyte activation.

CircSTRN3 in M1-Exos Promoted A1 Astrocytes Activation

To explore which circRNA functions in M1-exos, we performed RNA sequencing for M1-exos. Based on the sequencing results, 8 circRNAs were observed to be upregulated in M1-exos (Figure 3A). Notably, among these circRNAs, only circSTRN3 has been reported to demonstrate a positive association with inflammation.³¹ Then, we found circSTRN3 expressed in both primary microglia and astrocytes. After OGD/R, circSTRN3 was found increased in microglia and astrocytes (Figure 3B). The qRT-PCR analysis showed the expression level of circSTRN3 was higher in M1-exos than in M0-exos (Figure 3C). After adding the medium supernatant and exosomes from M1 microglia to primary astrocytes respectively, the expression of circSTRN3 in the astrocytes was up-regulated (Figure 3D and E). Transfection of overexpressed circSTRN3 (OE-circSTRN3) promoted furtherly activation and upregulation of NF-κB pathway and C3 expression after OGD/R (Figure 3F–I). All the primer sequences for qRT-PCR were shown in Supplementary Table S1. These results manifested that circSTRN3 in M1-exos promoted the activation of A1 astrocytes.

MiR-331-5p Could Be Bound to circSTRN3

In order to verify which miRNA circSTRN3 sponged to affect the activation of A1 astrocytes, we searched the bioinformatics prediction website (<https://bibiserv.cebitec.unibielefeld.de/rna>). We found that miR-331-5p could be bound to circSTRN3 (Figure 4A) and the dual-luciferase reporter assay proved the combination of miR-331-5p and circSTRN3 (Figure 4B). Then, we transfected miR-331-5p mimic and inhibitor to astrocytes respectively to verified their

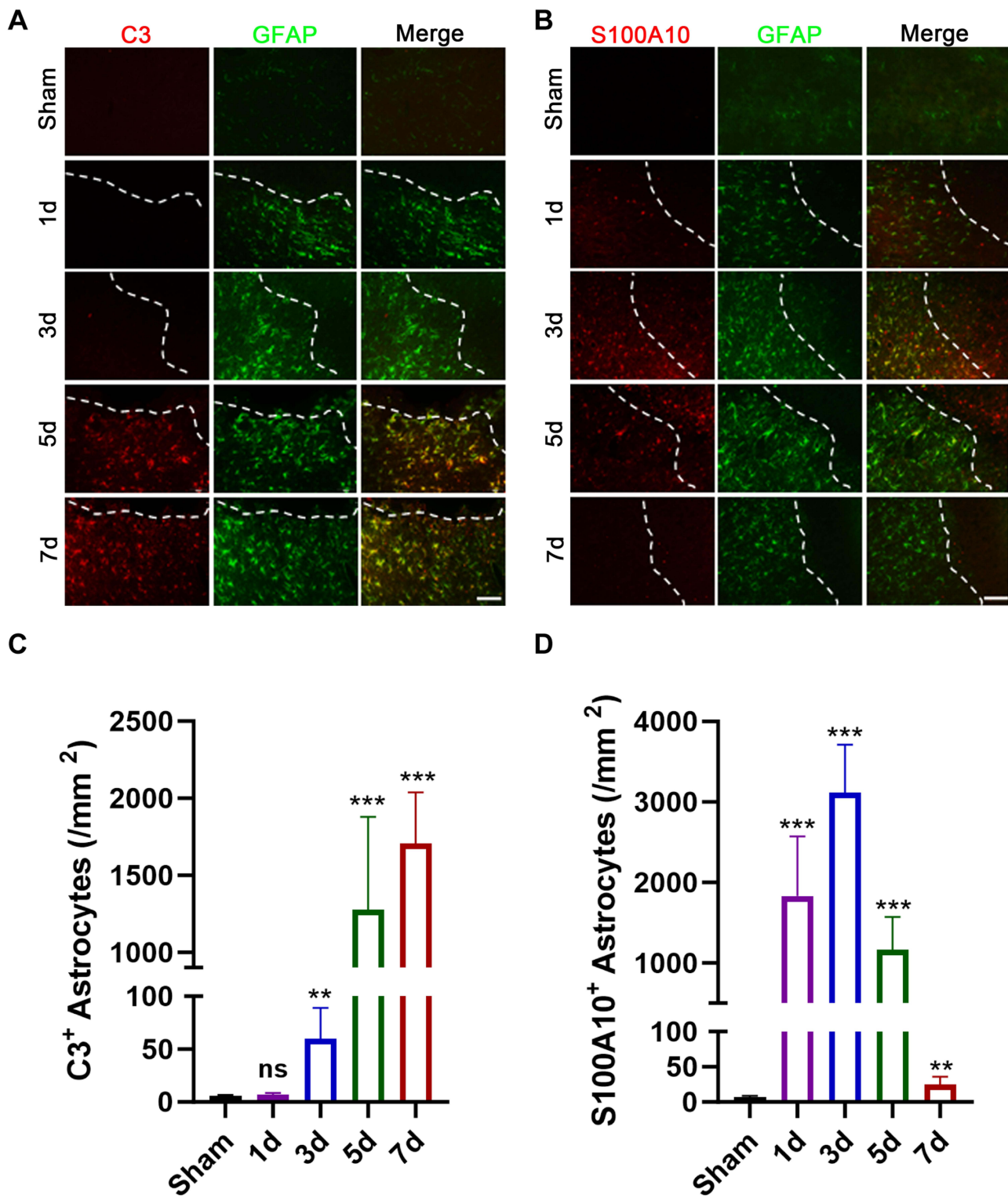


Figure 1 The polarization of A1 and A2 astrocytes by immunofluorescence images at various time points after MCAO/R models. **(A)** The fluorescence intensity of A1 activation marker C3 in astrocytes was measured at 1, 3, 5 and 7 days after MCAO/R. **(B)** The fluorescence intensity of A2 activation marker S100A10 in astrocytes was measured at 1, 3, 5 and 7 days after MCAO/R. **(C)** The quantitative analysis for C3-positive astrocytes (per mm²) in images of **(A)**. **(D)** The quantitative analysis for S100A10-positive astrocytes (per mm²) in images of **(B)**. Data were represented as mean ± SD. ***P* < 0.01; ****P* < 0.001 and “ns” for comparison with Sham group. The “ns” stands for no statistical significance. MCAO/R, middle cerebral artery occlusion/reperfusion. Scale bar: 50 μm.

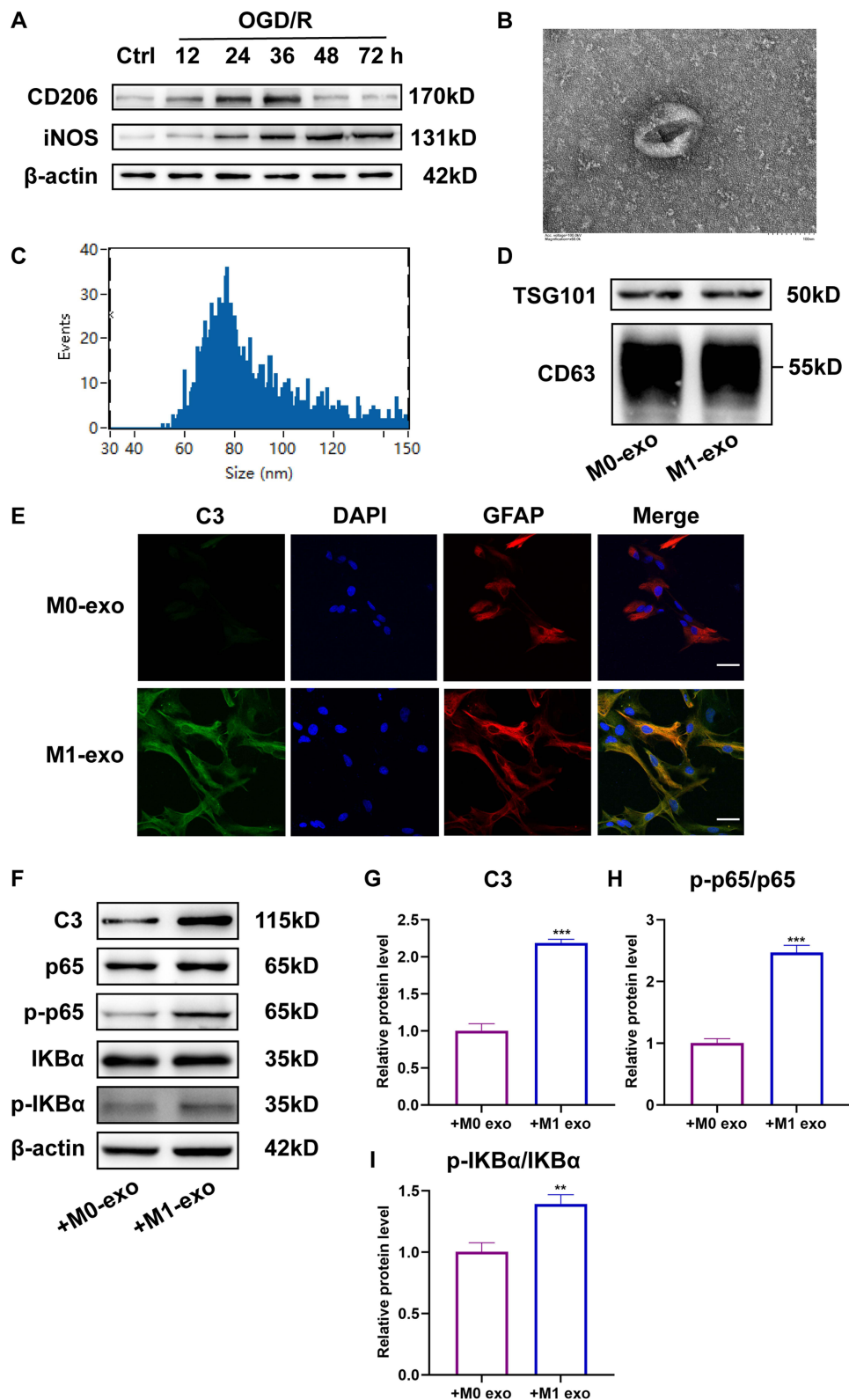


Figure 2 Exosomes from OGD/R-induced M1 microglia stimulated the activation of AI astrocytes. **(A)** The expression of iNOS (M1 marker) and CD206 (M2 marker) by WB in microglia at different time points after OGD/R. **(B)** Representative electron microscope images of microglia-derived exosomes. Scale bar: 100 nm. **(C)** The NTA described size distribution patterns of exosomes. **(D)** The detection of exosome markers TSG101 and CD63 by WB. **(E)** Immunofluorescence images of astrocytes after adding M0-exos and M1-exos severally. Scale bar: 20 μ m. **(F)** The influence of M0-exos and M1-exos on C3 and NF- κ B pathway in astrocytes by WB (n = 3). **(G–I)** The quantitative analysis of WB images in **(F)**. Data were represented as mean \pm SD. ** $p < 0.01$; *** $p < 0.001$ for Astrocytes + M1-exo group vs Astrocytes + M0-exo group. M0-exos referred to exosomes isolated from microglia under Standard cell culture conditions. M1-exos referred to exosomes isolated from OGD/R microglia. **Abbreviations:** OGD/R, oxygen-glucose deprivation/reperfusion model; NTA, nanoparticle tracking analysis; WB, Western blot.

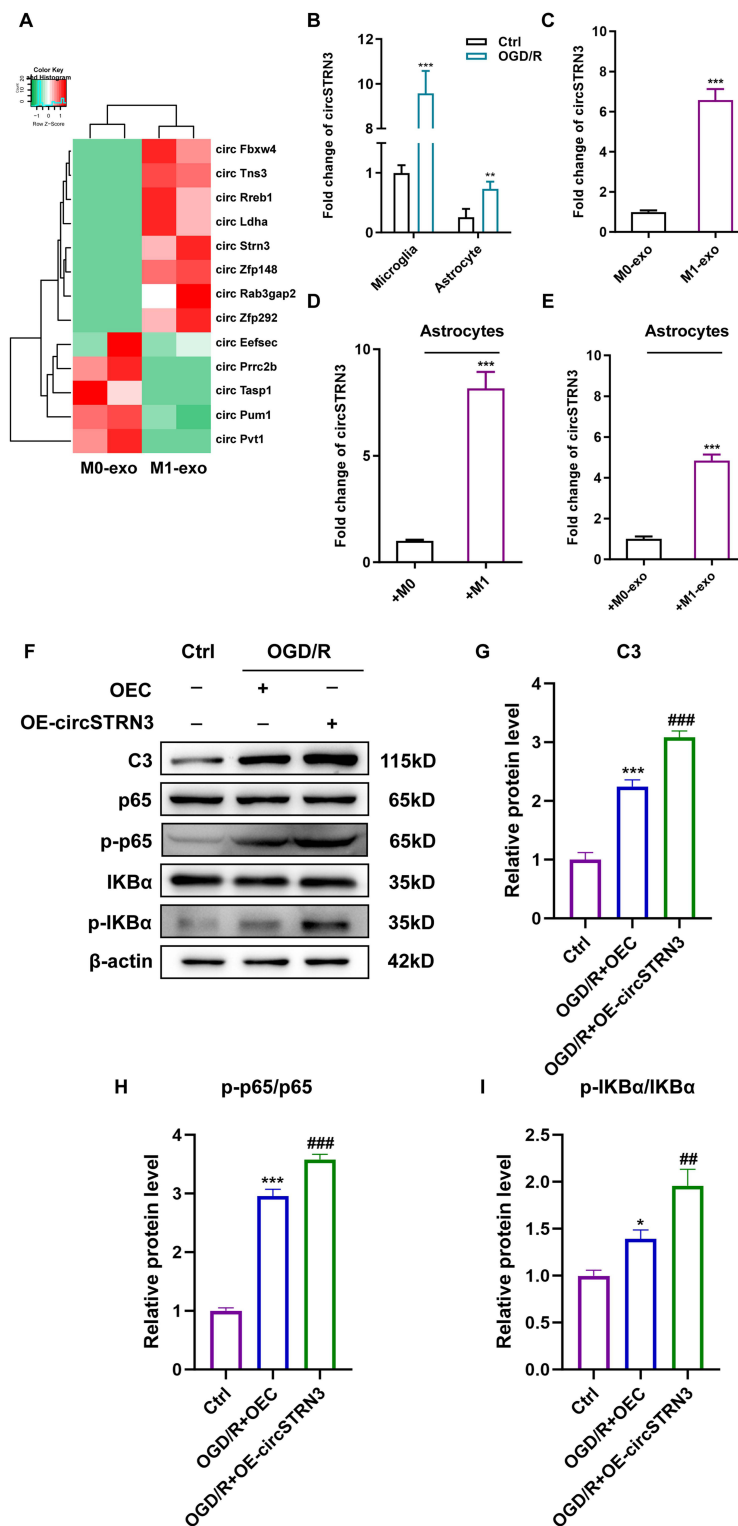


Figure 3 CircSTRN3 in M1-exos promoted astrocyte activation. (A) The heat map exhibited the sequencing results of M0-exos and M1-exos. Red represents up-regulation while green stands for down-regulation. (B–E) The expression of circSTRN3 detected by qRT-PCR analysis in microglia and astrocytes after OGD/R (B), in M0-exos and M1-exos (C), in astrocytes with the addition of M0 or M1 supernatant (D) and in astrocytes after adding M0-exos or M1-exos (E). ** $P < 0.01$; *** $P < 0.001$ for OGD/R group vs Control group, M1-exo group vs M0-exo group, Astrocytes + M1 group vs Astrocytes + M0 group, Astrocytes + M1-exo group vs Astrocytes + M0-exo group. (F) The influence of OE-circSTRN3 on C3 and NF- κ B pathway in astrocytes after OGD/R by WB. (G–I) The quantitative analysis of WB images in (F). Data were represented as mean \pm SD. * $P < 0.05$; *** $P < 0.001$ for OGD/R + OEC group vs Control group. ### $P < 0.01$; #### $P < 0.001$ for OGD/R + OE-circSTRN3 group vs OGD/R + OEC group. M0 represented microglia under Standard cell culture conditions while M1 was those underwent OGD/R. M0-exos were exosomes isolated from M0. M1-exos were exosomes derived from M1.

Abbreviations: OGD/R, oxygen-glucose deprivation/reperfusion model; qRT-PCR, quantitative real-time polymerase chain reaction; WB, Western blot.

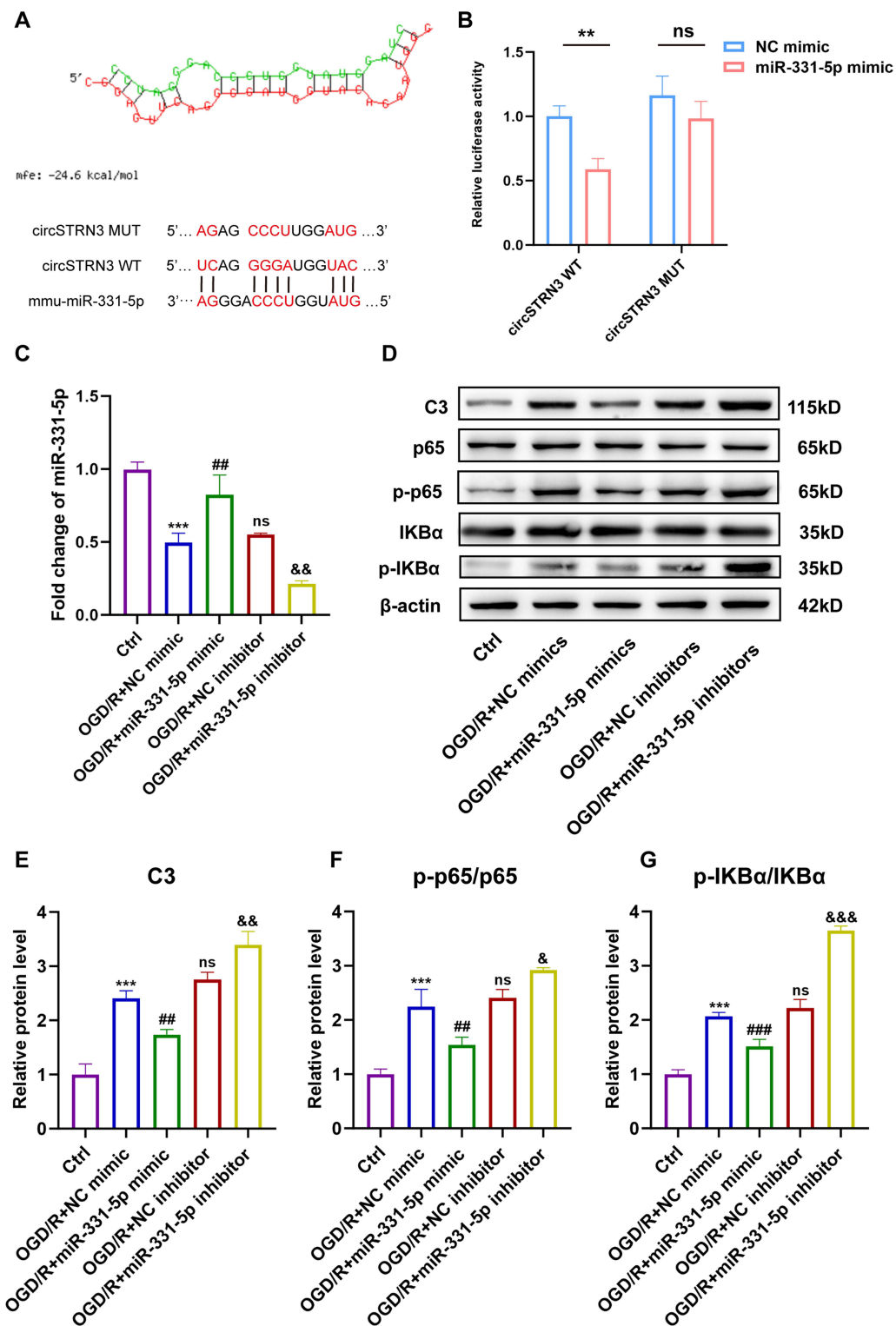


Figure 4 MiR-331-5p could be bound to circSTRN3 and regulate the AI astrocyte activation. **(A)** The bioinformatics prediction website (<https://bibiserv.cebitec.uni-bielefeld.de/rna>) identified the possible binding sites of circSTRN3 and miR-331-5p. **(B)** Relative luciferase activity of circSTRN3 wild-type and 3'-UTR mutant structures transfected with miR-331-5p mimic and NC mimic. $**P < 0.01$ for NC mimic group vs miR-331-5p mimic group; "ns" stands for no statistical significance. **(C)** The transfection efficiency of miR-331-5p mimic and inhibitor in astrocytes performed by WB after OGD/R ($n = 3$). **(D)** The regulation of miR-331-5p mimic and inhibitor on C3 and NF- κ B pathway in astrocytes by WB after OGD/R ($n = 3$). **(E–G)** The quantitative analysis for WB images in **(D)**. Data were represented as mean \pm SD. $***P < 0.001$ for OGD/R + NC mimic group vs Control group. $###P < 0.01$; $####P < 0.001$ for OGD/R + miR-331-5p mimic group vs OGD/R + NC mimic group. The "ns" represents no statistical significance between OGD/R + NC mimic group and OGD/R + NC inhibitor group. $^{\#}p < 0.05$; $^{\&}p < 0.01$; $^{\&\&}p < 0.001$ for OGD/R + miR-331-5p inhibitor group vs OGD/R + NC inhibitor group.

Abbreviations: WB, Western blot; OGD/R, oxygen-glucose deprivation/reperfusion model.

efficiency (Figure 4C). Under OGD/R, miR-331-5p mimic could suppress the NF- κ B pathway and C3 while miR-331-5p inhibitors promoted the A1 astrocyte activation ulteriorly (Figure 4C–G). The results indicated that miR-331-5p was a spongy target of circSTRN3 for the activation of A1 astrocytes.

CircSTRN3 Activated A1 Astrocytes Through Regulating miR-331-5p

To furtherly determine circSTRN3 sponged miR-331-5p to take part in the A1 astrocyte activation, we first detected the effect of transfecting OE-circSTRN3 on miR-331-5p in astrocytes. The qRT-PCR results revealed that OE-circSTRN3 induced down-regulation of miR-331-5p was reversed by miR-331-5p mimics after OGD/R (Figure 5A). Furthermore, miR-331-5p mimic abated the up-regulated protein expression of NF- κ B pathway and C3 caused by circSTRN3 in astrocytes (Figure 5B–E). Overall, these results indicated circSTRN3 promoted the activation of A1 astrocytes through miR-331-5p.

MiR-331-5p Regulated A1 Astrocytes Activation Through MAVS

To explore which mRNA was the target of miR-331-5p in astrocytes, we searched the prediction website (www.targetscan.org) and found that MAVS could be bound to miR-331-5p (Figure 6A). The combination of miR-331-5p and MAVS was confirmed by the dual-luciferase reporter assay (Figure 6B). Compared to NC mimic, miR-331-5p mimic decreased the protein expression of MAVS after OGD/R, while miR-331-5p inhibitor increased it when comparing to NC inhibitor (Figure 6C and D). Meanwhile, the overexpressed MAVS (OE-MAVS) reversed the decrement of NF- κ B pathway and C3 caused by miR-331-5p mimic after OGD/R (Figure 6E–H). These findings suggested that miR-331-5p targeted on MAVS, thereby potentiating the A1 astrocyte activation.

CircSTRN3 Promoted the A1 Astrocyte Activation Through miR-331-5p/MAVS/NF- κ B Axis in MCAO/R Models

To confirm whether circSTRN3 promoted the activation of A1 astrocytes in mice, we constructed MCAO/R models. Compared to MCAO/R group, OE-circSTRN3 aggravated the neurological impairment in MCAO/R mice according to mNSS, corner test and rotarod test while miR-331-5p mimic reversed the effect (Figure 7A–C). Similarly, OE-circSTRN3 increased the infarction size and promoted cell death in MCAO/R mice, while miR-331-5p mimic reversed it (Figure 7D–F). According to qRT-PCR results, the reduced expression of miR-331-5p induced by OE-circSTRN3 was reversed by miR-331-5p mimic in MCAO/R mice (Figure 7G). As WB results showed, OE-circSTRN3 furtherly increased the expression of MAVS, NF- κ B pathway and C3 in MCAO/R mice, while miR-331-5p mimic abolished the effect (Figure 7H–L). These results verified circSTRN3 was capable of enhancing the A1 astrocyte activation in mice models by targeting the miR-331-5p/MAVS/NF- κ B signaling pathway.

Correlation of circSTRN3 and miR-331-5p in the Exosomes from Peripheral Blood of IS Patients

To validate the expression of circSTRN3 and miR-331-5p in IS patients, we collected peripheral blood from 30 IS patients and 30 HC and extracted exosomes. The demographic and clinical characteristics of participants were shown in [Supplementary Table S2](#). The qRT-PCR analysis revealed that the expression of circSTRN3 was higher in IS patients than in HC (Figure 8A). Conversely, the expression of miR-331-5p was down-regulated in IS patients compared to HC (Figure 8B). Furthermore, we explored the potential relationships between circSTRN3, miR-331-5p and NIHSS on admission, which represented the severity of stroke. Our study demonstrated a negative correlation between circSTRN3 and miR-331-5p expression in stroke patients (Figure 8C). Additionally, CircSTRN3 expression positively correlated with NIHSS, while miR-331-5p expression negatively correlated with it (Figure 8D and E). These findings were consistent with our previous observations in cellular and animal models, suggesting that circSTRN3 and miR-331-5p exhibit an inverse relationship in IS patients.

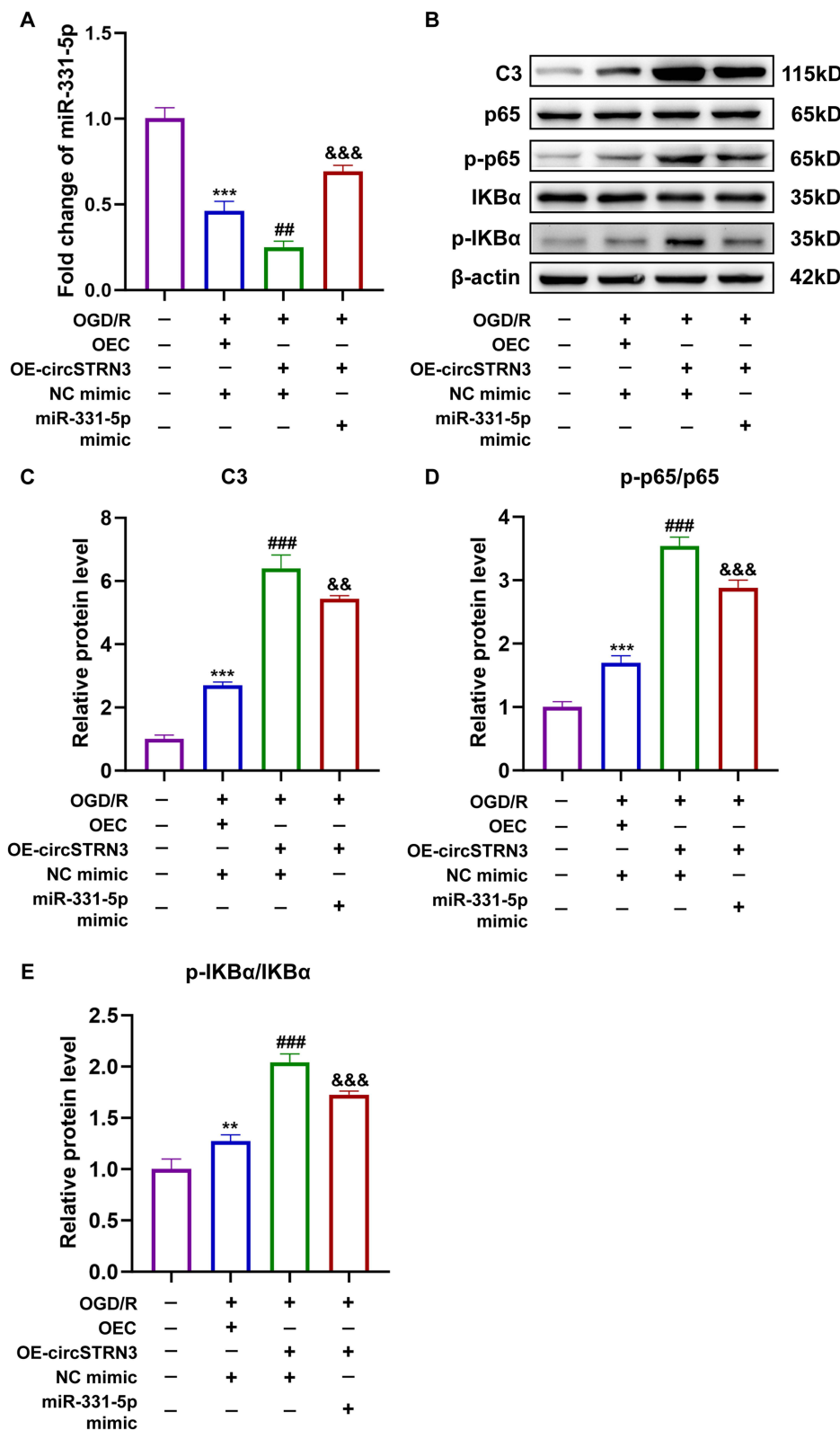


Figure 5 CircSTRN3 promoted A1 astrocyte activation via sponging miR-331-5p. **(A)** The influence of circSTRN3 and miR-331-5p mimic on miR-331-5p expression in astrocytes by qRT-PCR analysis under OGD/R (n = 3). **(B)** CircSTRN3 sponged miR-331-5p to affect C3 and NF-κB pathway expression in astrocytes by WB under OGD/R (n = 3). **(C–E)** The quantitative analysis of WB images in **(B)**. Data were represented as mean ± SD. **P < 0.01; ***P < 0.001 for OGD/R + OEC + NC mimic group vs Control group. ###P < 0.01; ####P < 0.001 for OGD/R + OE-circSTRN3 + NC mimic group vs OGD/R + OEC + NC mimic group. &&P < 0.01; &&&P < 0.001 for OGD/R + OE-circSTRN3 + miR-331-5p mimic group vs OGD/R + OE-circSTRN3 + NC mimic group.

Abbreviations: qRT-PCR, quantitative real-time polymerase chain reaction; WB, Western blot; OGD/R, oxygen-glucose deprivation/reperfusion model; OEC, over-expressed lentivirus control.

Discussion

Initially, our research confirmed that M1 microglia underwent activation prior to A1 astrocytes after MCAO/R. Subsequently, we revealed that A1 astrocyte activation could be mediated by M1-exos through cell experiments. The exosome sequencing results suggested that circSTRN3 enriched in M1-exos. We delved deeper into the mechanism in OGD/R models, revealing that circSTRN3 acts as a sponge for miR-331-5p, thereby facilitating the activation of A1 astrocytes through MAVS/NF- κ B axis. Following this, we reconfirmed this pathway in MCAO/R models. Finally, in patients with IS, circSTRN3 expression was up-regulated and positively correlated with NIHSS, indicating its potential role in promoting the severity of stroke symptoms.

Studies have demonstrated the pivotal role played by microglia and astrocytes in IS.⁴² After IS, reactive microglia and astrocytes become actively involved in modulating neuroinflammation, immune response, and BBB through pro-inflammatory and anti-inflammatory phenotypes.⁴³⁻⁴⁵ Previous studies have confirmed the activation of astrocytes and microglia was interrelated.^{46,47} Liddelow et al proved reactive microglia could activate A1 astrocytes by secreting inflammatory cytokines.⁴⁸ In our study, we verified M1 microglia were activated earlier than A1 astrocytes after ischemic injury.

In IS, exosomes were considered to be a promising biomarker of stroke prognosis for their association with angiogenesis, neurogenesis, autophagy and integrity of BBB.^{49,50} Previous studies showed a significant role of microglia-derived exosomes

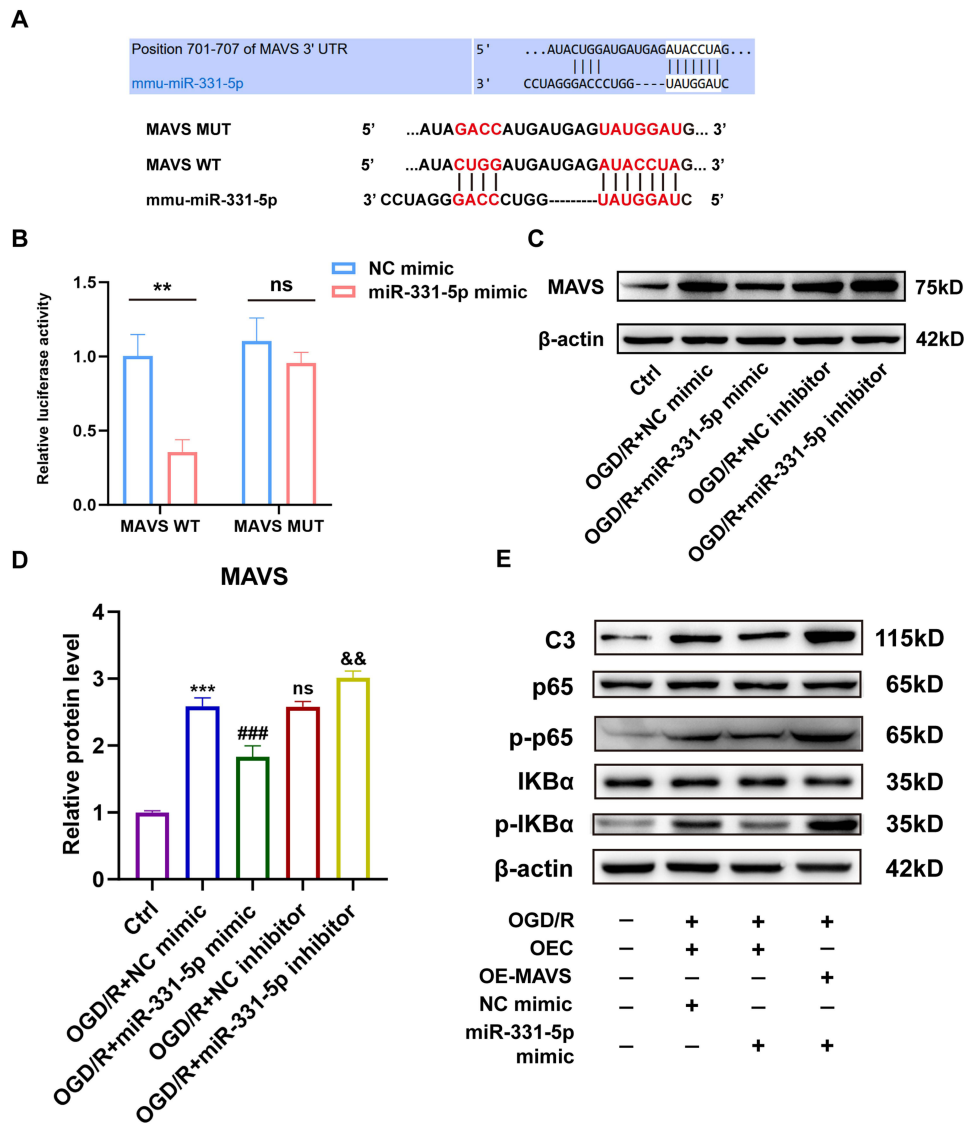


Figure 6 Continued.

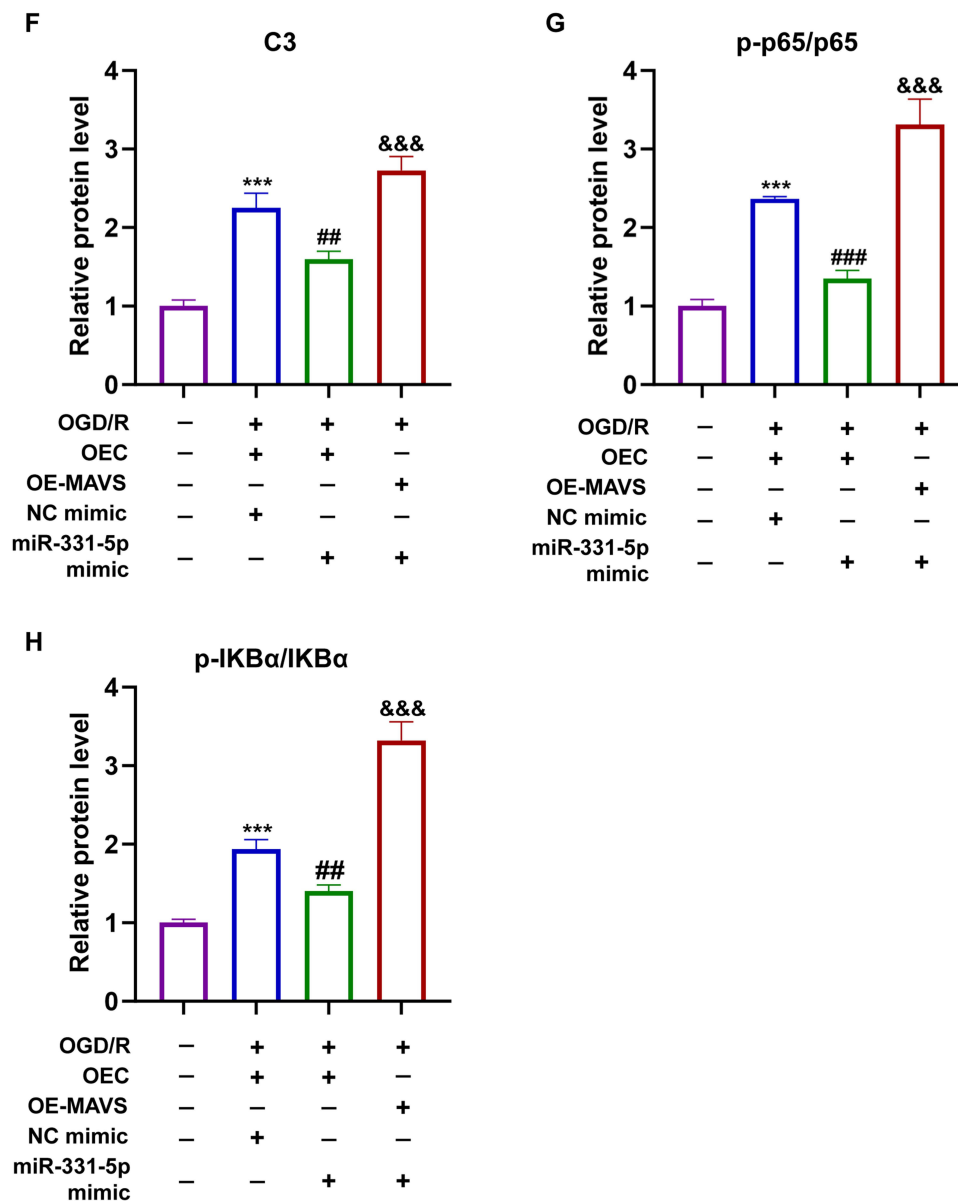


Figure 6 MiR-331-5p regulated the activation of A1 astrocytes through MAVS. **(A)** The predictive binding sites of miR-331-5p and MAVS according to https://www.targetscan.org/vert_80. **(B)** Relative luciferase activity of MAVS wild-type and 3'-UTR mutant structures transfected with miR-331-5p mimic and NC mimic. $^{**}P < 0.01$; "ns" stands for no statistical significance. **(C)** The miR-331-5p mimic and inhibitor could influence the protein expression of MAVS by WB (n = 3). **(D)** The quantitative analysis of WB images in **(C)**. $^{***}P < 0.001$ for OGD/R+NC mimic group vs Control group. $^{####}P < 0.001$ for OGD/R + miR-331-5p mimic group vs OGD/R + NC mimic group. The "ns" stands for no significance between OGD/R + NC inhibitor group and OGD/R + NC mimic group. $^{**}P < 0.01$ for OGD/R + miR-331-5p inhibitor group vs OGD/R + NC inhibitor group. **(E)** MiR-331-5p influenced MAVS to enhance C3 and NF- κ B pathway expression in astrocytes by WB under OGD/R (n = 3). **(F–H)** The quantitative analysis of WB images in **(E)**. Data were represented as mean \pm SD. $^{***}P < 0.001$ for OGD/R + NC mimic + OEC group vs Control group. $^{###}P < 0.01$; $^{####}P < 0.001$ for OGD/R + miR-331-5p mimic + OEC group vs OGD/R + NC mimic + OEC group. $^{***}P < 0.001$ for OGD/R + miR-331-5p mimic + OE-MAVS group vs OGD/R group + miR-331-5p mimic + OEC group.

in the development and prognosis of stroke.⁵¹ M2-exos, for instance, were reported to be conducive to neuronal protection and inhibiting neuronal pyroptosis.⁵² In addition, Gao et al demonstrated M1-exos could promote the ferroptosis in neuronal cells and increase neuronal damage.⁵³ In our study, we proved M1-exos triggered the A1 astrocyte activation, potentially exacerbating the neuroinflammation after ischemic injury.

CircRNAs have been proposed to play a role in oxidative stress and vascular endothelial dysfunction, potentially serving as potential biomarker candidates for IS.^{54,55} Furthermore, CircRNAs have been shown to be involved in the activation, autophagy, and apoptosis of astrocytes, thereby modulating the prognosis of IS. For example, downgrade

circCDC14A could relieve the activation of astrocytes and improve brain injury after IS.⁵⁶ CircHECTD1 could facilitate the autophagy of astrocytes after stroke by targeting miR-142. Knocking down circHECTD1 could ameliorate the astrocyte activation and ischemic injury.⁵⁷ CircCNOT6L was capable to decrease the apoptosis of astrocytes and hypoxia injury after stroke via miR99a-5p.⁵⁸ Prior studies have showed circSTRN3 could aggravate the LPS-induced

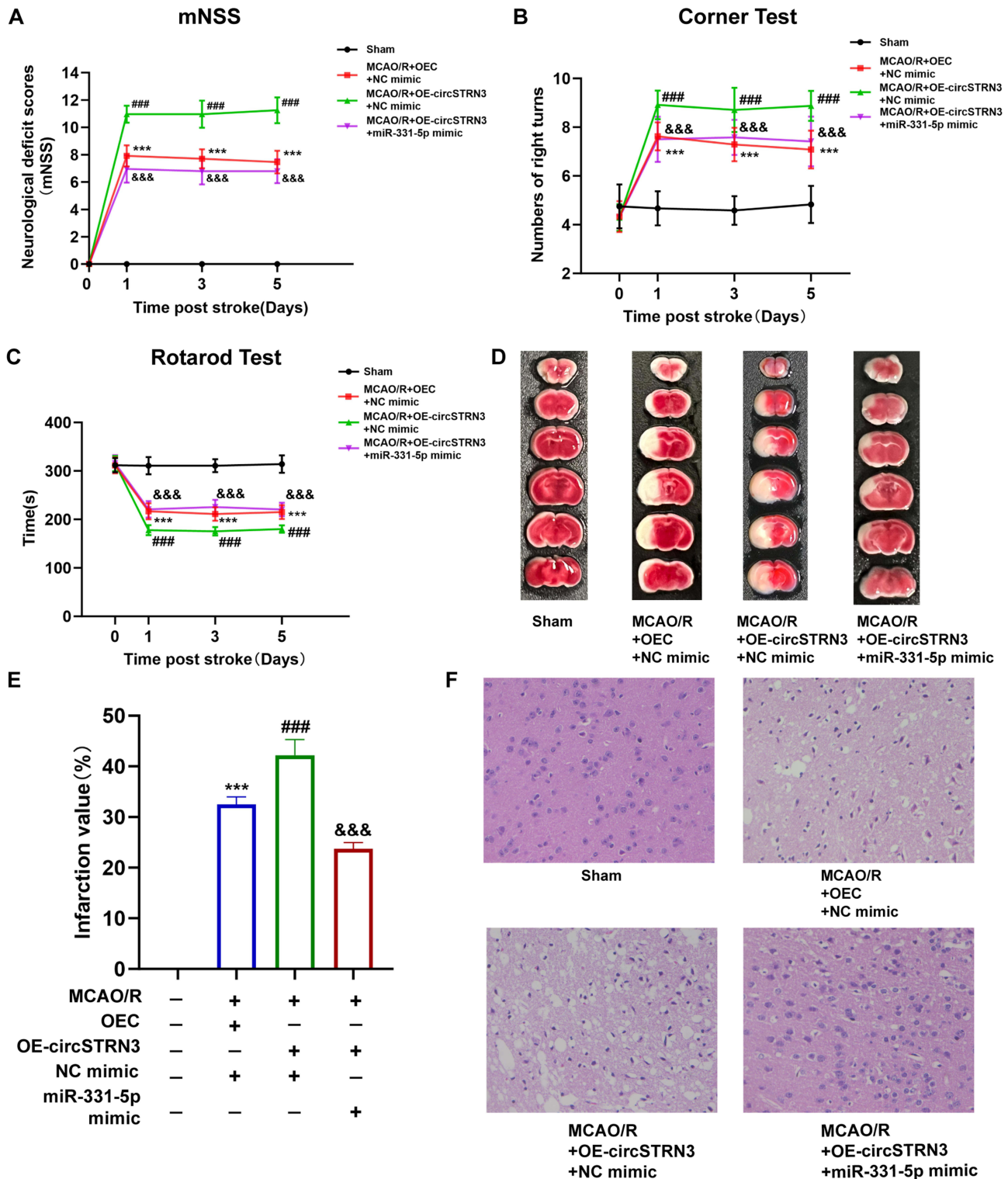


Figure 7 Continued.

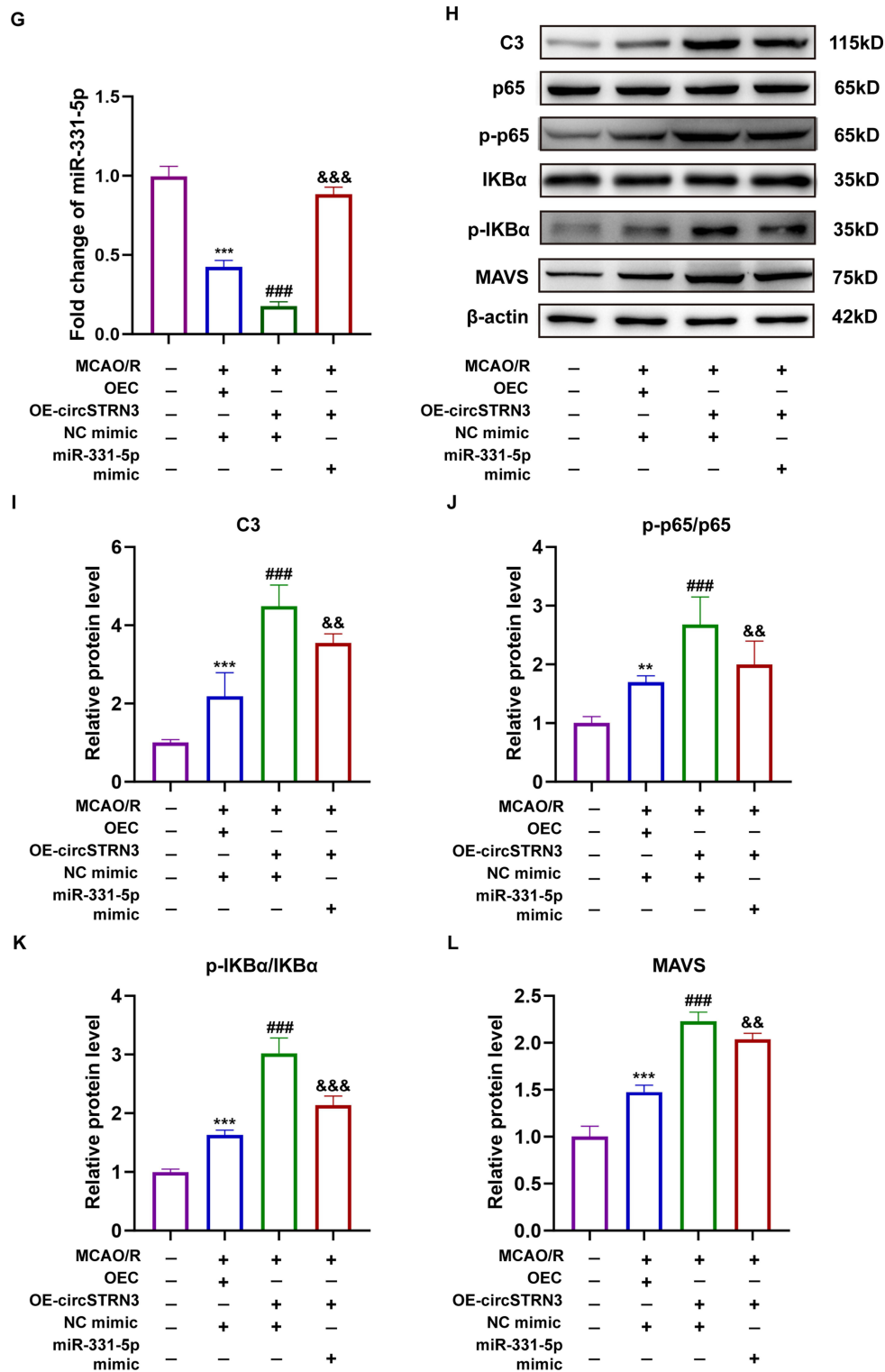


Figure 7 CircSTRN3 promoted the A1 astrocyte activation through miR-331-5p/MAVS/NF-κB axis in mice MCAO/R models. (A–C) The neural function and motor deficits of 4 mice groups (Sham, MCAO/R + OEC + NC mimic, MCAO/R + OE-circSTRN3 + NC mimic and MCAO/R + OE-circSTRN3 + miR-331-5p mimic) were evaluated by mNSS (A), corner test (B) and rotarod test (C) before MCAO/R (0 d) and 1, 3 or 5 days after MCAO/R (n = 24). (D and E) The infarction size of 4 groups were visualized through TTC staining (n = 6). (F) The infarction pathology of 4 groups were performed by HE staining (n = 6). (G) The alteration of miR-331-5p in brain tissues of 4 mice groups were tested by qRT-PCR (n = 6). (H) The expression of NF-κB pathway, C3 and MAVS in 4 groups were detected by WB (n = 6). (I–L) The quantitative analysis of WB images in (H). Data were represented as mean ± SD. ***P* < 0.01; ****P* < 0.001 for MCAO/R + OEC + NC mimic group vs Sham group. ####*P* < 0.001 for MCAO/R + OE-circSTRN3 + NC mimic group vs MCAO/R + OEC + NC mimic group. &&*P* < 0.01; &&&*P* < 0.001 for MCAO/R + OE-circSTRN3 + miR-331-5p mimic group vs MCAO/R + OE-circSTRN3 + NC mimic group.

Abbreviations: MCAO/R, middle cerebral artery occlusion/reperfusion; mNSS, modified neurological severity score; TTC staining, 2,3,5-Triphenyltetrazolium chloride staining; HE staining, hematoxylin-eosin staining; WB, Western blot; qRT-PCR, quantitative real-time polymerase chain reaction; OEC, overexpressed lentivirus control.

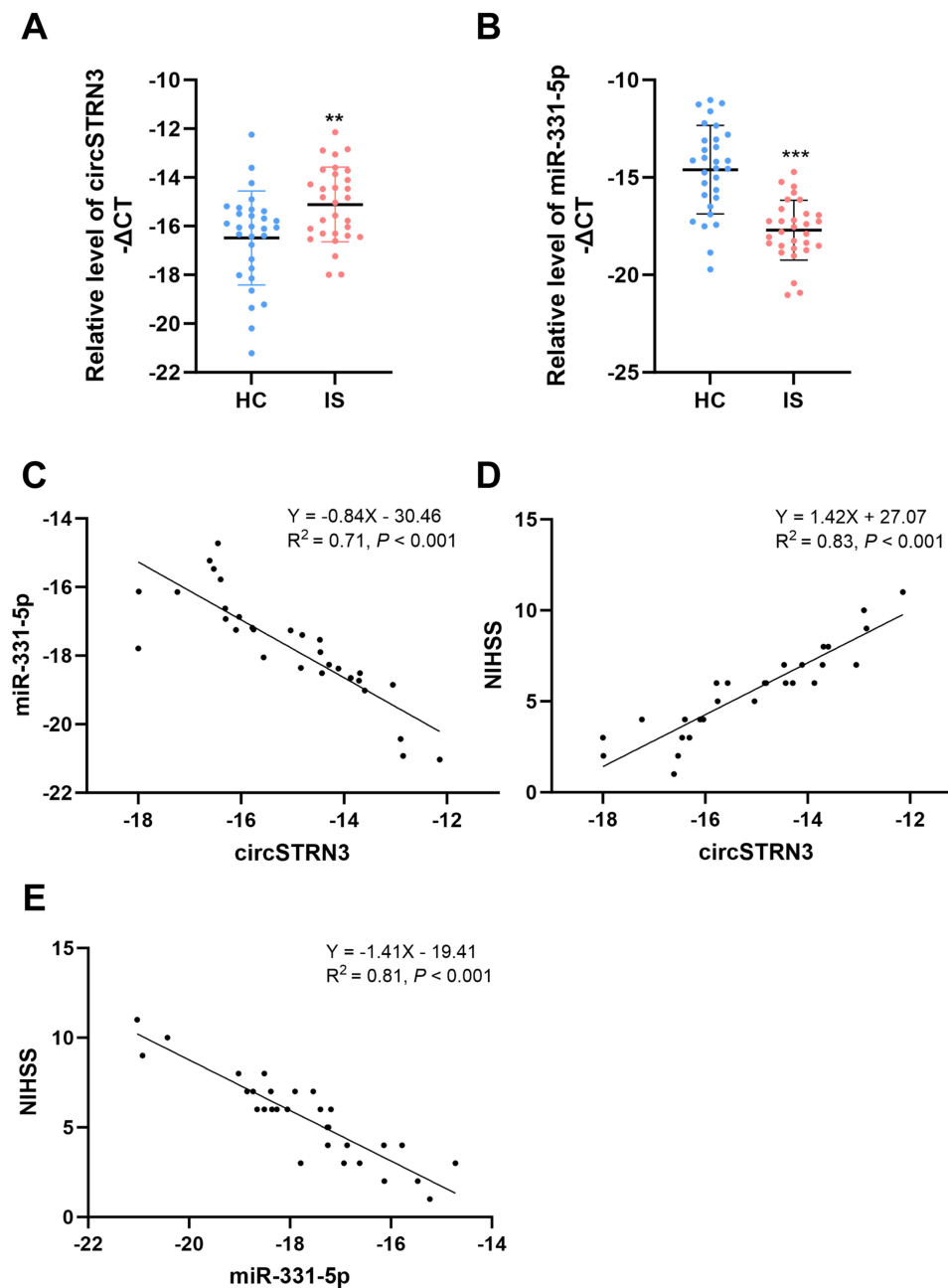


Figure 8 The expression levels and correlation of circSTRN3 and miR-331-5p in the exosomes derived from peripheral blood samples of IS patients. **(A and B)** CircSTRN3 **(A)** and miR-331-5p **(B)** expression levels in IS patients comparing to HC by qRT-PCR analysis. **(C)** The correlation of circSTRN3 and miR-331-5p in IS patients by Pearson correlation analysis. **(D)** The correlation analysis between NIHSS on admission and circSTRN3. **(E)** The correlation analysis between NIHSS on admission and miR-331-5p. The number of HC and IS patients was 30 to 30. Data were represented as mean \pm SD. ** $P < 0.01$; *** $P < 0.001$ for IS group vs HC group. The RNA expression levels were represented by the value of $-\Delta\text{CT}$.

Abbreviations: IS, ischemic stroke; HC, health control; qRT-PCR, quantitative real-time polymerase chain reaction; NIHSS, National Institute of Health stroke scale.

inflammatory injury,⁵⁹ while the effect on stroke remains unknown. Our study detected that circSTRN3 could aggravate the ischemic injury via facilitating the A1 astrocyte activation.

For circRNAs could sponge miRNAs to take effect, the current researches have also recognized miRNAs as potential therapeutic targets of IS. For example, Taylor et al found decreased miR-20a-3p was correlated with severe stroke outcomes in rats. Overexpressed miR-20a-3p could decrease infarct volume and improved neural functions.⁶⁰ Ge et al found inhibiting miR-19a contributed to protecting neurons against ischemic injury through regulating neuronal apoptosis.⁶¹ Song et al found miR-124 could enhance neural stem cell proliferation to facilitate functional recovery after IS.⁶² MiR-331-5p was reported to

alleviate the neurological deficits and inflammasome activation after IS.³² Furtherly, our research indicated miR-331-5p participated in the neuroinflammation after stroke through regulating the A1 astrocyte activation.

In the previous studies, MAVS was expected to be a critical target for immune response, inflammation and cell metabolic function.⁶³ MAVS was reported to have a crucial function in various diseases such as renal diseases,⁶⁴ cancer⁶⁵ and cardiovascular diseases.⁶⁶ It was also noted that MAVS took part in activating astrocytes via NF- κ B pathway and influencing neuroinflammation.¹⁸ Similarly, our research showed the activation of MAVS/NF- κ B axis after IS took effect in A1 astrocyte activation and aggravated ischemic injury.

Certainly, our research endeavored inherently encompass certain constraints, particularly the inability to utilize laser Doppler technology for quantifying cerebral blood flow in MCAO mice owing to resource constraints, a factor that might subtly influence the outcomes. As we progress, we are committed to refining this aspect in our upcoming experimental endeavors.

Conclusion

In summary, our research has yielded fresh evidence demonstrating that circSTRN3, derived from M1-exos, can target the miR-331-5p/MAVS/NF- κ B pathway to facilitate the A1 astrocyte activation following IS. This discovery offers a deeper understanding into the potential mechanisms of these molecules in the development of IS, thereby contributing to the advancement of therapeutic strategies.

Data Sharing Statement

The datasets used and/or analyzed during the current study are available from the corresponding author on reasonable request.

Ethics Approval and Consent to Participate

The study was conducted in accordance with the Declaration of Helsinki, and approved by the Ethics Committee of Nanjing First Hospital (Approval No. KY20211011-05). The animal study protocol was approved by the Ethics Committee of Nanjing First Hospital (Approval No. DWSY-23146450).

Author Contributions

All authors made a significant contribution to the work reported, whether that is in the conception, study design, execution, acquisition of data, analysis and interpretation, or in all these areas; took part in drafting, revising or critically reviewing the article; gave final approval of the version to be published; have agreed on the journal to which the article has been submitted; and agree to be accountable for all aspects of the work.

Funding

This study was supported by the National Natural Science Foundation of China (No. 82201460) and China Postdoctoral Science Foundation (No. 2023M731744).

Disclosure

The authors declare no potential conflicts of interest.

References

1. Feigin VL, Nguyen G, Cercy K, et al. Global, regional, and country-specific lifetime risks of stroke, 1990 and 2016. *N Engl J Med.* 2018;379(25):2429–2437.
2. Feigin VL, Stark BA, Johnson CO, et al. Global, regional, and national burden of stroke and its risk factors, 1990–2019: a systematic analysis for the Global Burden of Disease Study 2019. *Lancet Neurol.* 2021;20(10):795–820. doi:10.1016/S1474-4422(21)00252-0
3. Candelario-Jalil E, Dijkhuizen RM, Magnus T. Neuroinflammation, stroke, blood-brain barrier dysfunction, and imaging modalities. *Stroke.* 2022;53(5):1473–1486. doi:10.1161/STROKEAHA.122.036946
4. Cai W, Dai X, Chen J, et al. STAT6/Arg1 promotes microglia/macrophage efferocytosis and inflammation resolution in stroke mice. *JCI Insight.* 2019;4(20). doi:10.1172/jci.insight.131355
5. Stonesifer C, Corey S, Ghanekar S, Diamandis Z, Acosta SA, Borlongan CV. Stem cell therapy for abrogating stroke-induced neuroinflammation and relevant secondary cell death mechanisms. *Prog Neurobiol.* 2017;158:94–131. doi:10.1016/j.pneurobio.2017.07.004

6. Anthony S, Cabantan D, Monsour M, Borlongan CV. Neuroinflammation, stem cells, and stroke. *Stroke*. 2022;53(5):1460–1472. doi:10.1161/STROKEAHA.121.036948
7. Qiu YM, Zhang CL, Chen AQ, et al. Immune cells in the BBB disruption after acute ischemic stroke: targets for immune therapy? *Front Immunol*. 2021;12:678744. doi:10.3389/fimmu.2021.678744
8. Xu S, Lu J, Shao A, Zhang JH, Zhang J. Glial cells: role of the immune response in ischemic stroke. *Front Immunol*. 2020;11:294.
9. Quan H, Zhang R. Microglial dynamic response and phenotype heterogeneity in neural regeneration following hypoxic-ischemic brain injury. *Front Immunol*. 2023;14:1320271.
10. Cheon SY, Kim EJ, Kim JM, Kam EH, Ko BW, Koo BN. Regulation of microglia and macrophage polarization via Apoptosis signal-regulating kinase 1 silencing after ischemic/hypoxic injury. *Front Mol Neurosci*. 2017;10:261.
11. Kobashi S, Terashima T, Katagi M, et al. Transplantation of M2-deviated microglia promotes recovery of motor function after spinal cord injury in mice. *Mol Ther*. 2020;28(1):254–265. doi:10.1016/j.yjth.2019.09.004
12. Zhang L, Zhang J, You Z. Switching of the microglial activation phenotype is a possible treatment for depression disorder. *Front Cell Neurosci*. 2018;12:306. doi:10.3389/fncel.2018.00306
13. Pepe G, Calderazzi G, De Maglie M, Villa AM, Vegeto E. Heterogeneous induction of microglia M2a phenotype by central administration of interleukin-4. *J Neuroinflammation*. 2014;11:211. doi:10.1186/s12974-014-0211-6
14. Hu X, Li P, Guo Y, et al. Microglia/macrophage polarization dynamics reveal novel mechanism of injury expansion after focal cerebral ischemia. *Stroke*. 2012;43(11):3063–3070. doi:10.1161/STROKEAHA.112.659656
15. Li S, Zhang R, Wang A, et al. Panax notoginseng: derived exosome-like nanoparticles attenuate ischemia reperfusion injury via altering microglia polarization. *J Nanobiotechnology*. 2023;21(1):416. doi:10.1186/s12951-023-02161-1
16. Verkhatsky A, Butt A, Li B, et al. Astrocytes in human central nervous system diseases: a frontier for new therapies. *Signal Transduct Target Ther*. 2023;8(1). doi:10.1038/s41392-023-01628-9
17. Liu L-R, Liu J-C, Bao J-S, Bai Q-Q, Wang G-Q. Interaction of microglia and astrocytes in the neurovascular unit. *Front Immunol*. 2020;11:1024.
18. Chao -C-C, Gutiérrez-Vázquez C, Rothhammer V, et al. Metabolic control of astrocyte pathogenic activity via cPLA2-MAVS. *Cell*. 2019;179(7):1483–1498.e1422. doi:10.1016/j.cell.2019.11.016
19. Raposo G, Stoorvogel W. Extracellular vesicles: exosomes, microvesicles, and friends. *J Cell Biol*. 2013;200(4):373–383. doi:10.1083/jcb.201211138
20. Mashouri L, Yousefi H, Aref AR, Ahadi AM, Molaei F, Alahari SK. Exosomes: composition, biogenesis, and mechanisms in cancer metastasis and drug resistance. *Mol Cancer*. 2019;18(1):75. doi:10.1186/s12943-019-0991-5
21. Doyle LM, Wang MZ. Overview of extracellular vesicles, their origin, composition, purpose, and methods for exosome isolation and analysis. *Cells*. 2019;8(7):727. doi:10.3390/cells8070727
22. Chen C, Bao Y, Xing L, et al. Exosomes derived from M2 microglial cells modulated by 1070-nm light improve cognition in an Alzheimer's disease mouse model. *Adv Sci*. 2023;10(32). doi:10.1002/adv.202370223
23. Huber CC, Wang H. Pathogenic and therapeutic role of exosomes in neurodegenerative disorders. *Neural Regen Res*. 2024;19(1):75–79. doi:10.4103/1673-5374.375320
24. Wang M, Shu H, Cheng X, et al. Exosome as a crucial communicator between tumor microenvironment and gastric cancer (Review). *Int J Oncol*. 2024;64(3). doi:10.3892/ijo.2024.5616
25. Wang F, Jiang M, Chi Y, Huang G, Jin M. Exosomes from circRNA-Ptpn4 can modify ADSC treatment and repair nerve damage caused by cerebral infarction by shifting microglial M1/M2 polarization. *Mol Cell Biochem*. 2023;479:2081–2092.
26. Jeck WR, Sorrentino JA, Wang K, et al. Circular RNAs are abundant, conserved, and associated with ALU repeats. *RNA*. 2013;19(2):141–157. doi:10.1261/rna.035667.112
27. Yang R, Yang B, Liu W, Tan C, Chen H, Wang X. Emerging role of non-coding RNAs in neuroinflammation mediated by microglia and astrocytes. *J Neuroinflammation*. 2023;20(1). doi:10.1186/s12974-023-02856-0
28. Chen LL. The expanding regulatory mechanisms and cellular functions of circular RNAs. *Nat Rev Mol Cell Biol*. 2020;21(8):475–490. doi:10.1038/s41580-020-0243-y
29. Hansen TB, Jensen TI, Clausen BH, et al. Natural RNA circles function as efficient microRNA sponges. *Nature*. 2013;495(7441):384–388. doi:10.1038/nature11993
30. Zhou D, Huang Z, Zhu X, Hong T, Zhao Y. Circular RNA 0025984 ameliorates ischemic stroke injury and protects astrocytes through miR-143-3p/TET1/ORP150 pathway. *Mol Neurobiol*. 2021;58(11):5937–5953. doi:10.1007/s12035-021-02486-8
31. Gao Q, Zheng Y, Wang H, Hou L, Hu X. circSTRN3 aggravates sepsis-induced acute kidney injury by regulating miR-578/ toll like receptor 4 axis. *Bioengineered*. 2022;13(5):11388–11401. doi:10.1080/21655979.2022.2061293
32. Zhang HS, Liu MF, Ji XY, Jiang CR, Li ZL, OuYang B. Gastrodin combined with rhynchophylline inhibits cerebral ischaemia-induced inflammasome activation via upregulating miR-21-5p and miR-331-5p. *Life Sci*. 2019;239:116935. doi:10.1016/j.lfs.2019.116935
33. Deng Y, Duan R, Ding W, et al. Astrocyte-derived exosomal nicotinamide phosphoribosyltransferase (Nampt) ameliorates ischemic stroke injury by targeting AMPK/mTOR signaling to induce autophagy. *Cell Death Dis*. 2022;13(12). doi:10.1038/s41419-022-05454-9
34. Hu J, Duan H, Zou J, et al. METTL3-dependent N6-methyladenosine modification is involved in berberine-mediated neuroprotection in ischemic stroke by enhancing the stability of NEAT1 in astrocytes. *Aging*. 2024;16(1):299–321. doi:10.18632/aging.205369
35. Thompson CA, Purushothaman A, Ramani VC, Vlodayky I, Sanderson RD. Heparanase regulates secretion, composition, and function of tumor cell-derived exosomes. *J Biol Chem*. 2013;288(14):10093–10099. doi:10.1074/jbc.C112.444562
36. Wei W, Li H, Deng Y, Zheng X, Zhou Y, Xue X. The combination of Alisma and Atractylodes ameliorates cerebral ischaemia/reperfusion injury by negatively regulating astrocyte-derived exosomal miR-200a-3p/141-3p by targeting SIRT1. *J Ethnopharmacol*. 2023;313:116597.
37. Rio DC, Ares M, Hannon GJ, Nilsen TW. Purification of RNA using TRIzol (TRI reagent). *Cold Spring Harb Protoc*. 2010;2010(6):pdb.prot5439. doi:10.1101/pdb.prot5439
38. Legnini I, Di Timoteo G, Rossi F, et al. Circ-ZNF609 is a circular RNA that can be translated and functions in myogenesis. *Mol Cell*. 2017;66(1):22–37.e29. doi:10.1016/j.molcel.2017.02.017
39. Li Y, Chopp M, Chen J, et al. Intrastriatal transplantation of bone marrow nonhematopoietic cells improves functional recovery after stroke in adult mice. *J Cereb Blood Flow Metab*. 2000;20(9):1311–1319. doi:10.1097/00004647-200009000-00006

40. Li Z, Song Y, He T, et al. M2 microglial small extracellular vesicles reduce glial scar formation via the miR-124/STAT3 pathway after ischemic stroke in mice. *Theranostics*. 2021;11(3):1232–1248. doi:10.7150/thno.48761
41. Hong Y, Lyu J, Zhu L, et al. High-frequency repetitive transcranial magnetic stimulation (rTMS) protects against ischemic stroke by inhibiting M1 microglia polarization through let-7b-5p/HMGA2/NF-κB signaling pathway. *BMC Neuro*. 2022;23(1). doi:10.1186/s12868-022-00735-7
42. Gong Z, Guo J, Liu B, et al. Mechanisms of immune response and cell death in ischemic stroke and their regulation by natural compounds. *Front Immunol*. 2024;14:1287857.
43. Lu W, Wen J. Crosstalk among glial cells in the blood-brain barrier injury after ischemic stroke. *Mol Neurobiol*. 2024:1–4.
44. Vainchtein ID, Molofsky AV. Astrocytes and microglia: in sickness and in health. *Trends Neurosci*. 2020;43(3):144–154. doi:10.1016/j.tins.2020.01.003
45. Wang D, Wang Y, Shi J, et al. Edaravone dextran alleviates ischemic injury and neuroinflammation by modulating microglial and astrocyte polarization while inhibiting leukocyte infiltration. *Int Immunopharmacol*. 2024;130:111700. doi:10.1016/j.intimp.2024.111700
46. Peng L, Ji Y, Li Y, You Y, Zhou Y. PRDX6-iPLA2 aggravates neuroinflammation after ischemic stroke via regulating astrocytes-induced M1 microglia. *Cell Commun Signal*. 2024;22(1):76. doi:10.1186/s12964-024-01476-2
47. Zhao X, Wang Z, Wang J, et al. Mesencephalic astrocyte-derived neurotrophic factor (MANF) alleviates cerebral ischemia/reperfusion injury in mice by regulating microglia polarization via A20/NF-κB pathway. *Int Immunopharmacol*. 2024;127:111396. doi:10.1016/j.intimp.2023.111396
48. Liddel SA, Guttenplan KA, Clarke LE, et al. Neurotoxic reactive astrocytes are induced by activated microglia. *Nature*. 2017;541(7638):481–487. doi:10.1038/nature21029
49. Lee EC, Ha TW, Lee D-H, et al. Utility of exosomes in ischemic and hemorrhagic stroke diagnosis and treatment. *Int J Mol Sci*. 2022;23(15):8367.
50. Osaid Z, Haider M, Hamoudi R, Harati R. Exosomes interactions with the blood–brain barrier: implications for cerebral disorders and therapeutics. *Int J Mol Sci*. 2023;24(21):15635. doi:10.3390/ijms242115635
51. Li SS, Wu JJ, Xing XX, et al. Focal ischemic stroke modifies microglia-derived exosomal miRNAs: potential role of mir-212-5p in neuronal protection and functional recovery. *Biol Res*. 2023;56(1):52. doi:10.1186/s40659-023-00458-x
52. Li Z, Pang Y, Hou L, et al. Exosomal OIP5-AS1 attenuates cerebral ischemia-reperfusion injury by negatively regulating TXNIP protein stability and inhibiting neuronal pyroptosis. *Int Immunopharmacol*. 2024;127:111310. doi:10.1016/j.intimp.2023.111310
53. Gao S, Jia S, Bai L, Li D, Meng C. Transcriptome analysis unveils that exosomes derived from M1-polarized microglia induce ferroptosis of neuronal cells. *Cells*. 2022;11(24):3956. doi:10.3390/cells11243956
54. Zhang X, Wan M, Min X, et al. Circular RNA as biomarkers for acute ischemic stroke: a systematic review and meta-analysis. *CNS Neurosci Ther*. 2023;29(8):2086–2100. doi:10.1111/ens.14220
55. Scicchitano P, Cortese F, Gesualdo M, et al. The role of endothelial dysfunction and oxidative stress in cerebrovascular diseases. *Free Radic Res*. 2019;53(6):579–595. doi:10.1080/10715762.2019.1620939
56. Zuo L, Xie J, Liu Y, Leng S, Zhang Z, Yan F. Down-regulation of circular RNA CDC14A peripherally ameliorates brain injury in acute phase of ischemic stroke. *J Neuroinflammation*. 2021;18(1):283. doi:10.1186/s12974-021-02333-6
57. Han B, Zhang Y, Zhang Y, et al. Novel insight into circular RNA HECTD1 in astrocyte activation via autophagy by targeting MIR142-TIPARP: implications for cerebral ischemic stroke. *Autophagy*. 2018;14(7):1164–1184. doi:10.1080/15548627.2018.1458173
58. He W, Gu L, Yang J, et al. Exosomal circCNOT6L regulates astrocyte apoptotic signals induced by hypoxia exposure through miR99a-5p/SERPINE1 and alleviates ischemic stroke injury. *Mol Neurobiol*. 2023;60(12):7118–7135. doi:10.1007/s12035-023-03518-1
59. Min XL, Jia WJ, Guo L, et al. Brain microvascular endothelial cell-derived exosomes transmitting circ_0000495 promote microglial M1-polarization and endothelial cell injury under hypoxia condition. *FASEB J*. 2024;38(2):e23387. doi:10.1096/fj.202301637R
60. Branyan TE, Selvamani A, Park MJ, et al. Functional assessment of stroke-induced regulation of miR-20a-3p and its role as a neuroprotectant. *Transl Stroke Res*. 2022;13(3):432–448. doi:10.1007/s12975-021-00945-x
61. Ge XL, Wang JL, Liu X, Zhang J, Liu C, Guo L. Inhibition of miR-19a protects neurons against ischemic stroke through modulating glucose metabolism and neuronal apoptosis. *Cell Mol Biol Lett*. 2019;24:37. doi:10.1186/s11658-019-0160-2
62. Song Y, Shi R, Liu Y, et al. M2 microglia extracellular vesicle miR-124 regulates neural stem cell differentiation in ischemic stroke via AAK1/NOTCH. *Stroke*. 2023;54(10):2629–2639. doi:10.1161/STROKEAHA.122.041611
63. Belgnaoui SM, Paz S, Hiscott J. Orchestrating the interferon antiviral response through the mitochondrial antiviral signaling (MAVS) adapter. *Curr Opin Immunol*. 2011;23(5):564–572. doi:10.1016/j.coi.2011.08.001
64. Wu M, Pei Z, Long G, Chen H, Jia Z, Xia W. Mitochondrial antiviral signaling protein: a potential therapeutic target in renal disease. *Front Immunol*. 2023;14:1266461. doi:10.3389/fimmu.2023.1266461
65. Zhang J, Li S, Zhang J, et al. Docetaxel resistance-derived LINC01085 contributes to the immunotherapy of hormone-independent prostate cancer by activating the STING/MAVS signaling pathway. *Cancer Lett*. 2022;545:215829. doi:10.1016/j.canlet.2022.215829
66. Wang Q, Sun Z, Cao S, et al. Reduced immunity regulator MAVS contributes to non-hypertrophic cardiac dysfunction by disturbing energy metabolism and mitochondrial homeostasis. *Front Immunol*. 2022;13:919038. doi:10.3389/fimmu.2022.919038